

# USING MODIFIED INDUSTRIAL ROBOTS TO EMULATE THE CONTACT DYNAMICS BEHAVIOR OF A SPACE MANIPULATOR

Xiangyang Zhang<sup>1</sup>, Dapeng Han<sup>1</sup>, \*Ou Ma<sup>2</sup>

<sup>1</sup> School of Aerospace Engineering, Tsinghua University, Tsinghua Yuan, Beijing 100084, China, E-mail: [xiangyangz@mail.tsinghua.edu.cn](mailto:xiangyangz@mail.tsinghua.edu.cn)

<sup>2</sup> Department of Mechanical and Aerospace Engineering, New Mexico State University, Las Cruces, NM 88003, USA, E-mail: [oma@mail.tsinghua.edu.cn](mailto:oma@mail.tsinghua.edu.cn)

## ABSTRACT

The most challenging and risky operations for a space manipulator are those involving physical contact. To ensure safe and reliable contact operations, each such robotic task must be carefully designed and verified before it is performed in space. This paper provides an overview of a hardware-in-the-loop (HIL) simulation system which is designed for verification of general contact tasks of a space manipulator. The system uses two industrial robots to emulate the dynamic behavior of the space manipulator and a payload handled by the space manipulator. Due to special requirements for HIL simulation, industrial robots cannot be used as is. The paper focuses on the discussion regarding how to modify the industrial robots to meet the basic requirements of HIL simulation. The proposed modifications are being implemented right now. The test work completed so far indicates that the alternated robots will meet the proposed requirements for HIL simulation.

## 1 INTRODUCTION

With the increasing activities for space exploration and satellite on-orbit servicing, space missions requiring physical contact (including low-speed

impact) become more common than ever. The most challenging and risky operations for a space manipulator are those involving physical contact. To ensure safe and reliable contact operations, each such task must be carefully designed and verified on the ground before it can be performed in space. However, physical testing of many contact tasks of a space manipulator at the whole arm level, especially a long manipulator handling large-mass payload, on the ground is extremely difficult or even impossible due to the gravity effect. Therefore, other verification methods were sought for complementing the difficult physical testing.

There are two general approaches available to complement physical testing of space manipulators, one being computer simulation and the other hardware-in-the-loop simulation. The former requires a high-fidelity contact dynamics model which is usually difficult to obtain and the model itself is very difficult to be validated against hardware testing. The latter is a hardware-in-the-loop (HIL) hybrid system combining both computer simulation and hardware test. The concept of such a general robotics-based contact dynamics simulation facility is illustrated by the diagram shown in Fig.1.

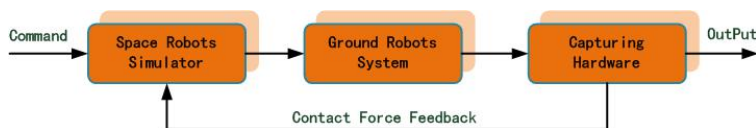


Figure 1: Three essential parts of an HIL contact dynamics simulator.

It uses a real-time computer to simulate the microgravity dynamics of the space manipulator; uses the simulation output to derive an industrial robot to emulate the dynamic behavior of the space robot and use real contact hardware to make physical contact; and then measures the resulting contact force and moment and feeds the force data back to the computer simulation of the space robot. The approach is an integration of real-time computer simulation and contact dynamics hardware test.

In fact, the approach of HIL simulation has been widely used to support the development and operations of space robotics and automation systems. NASA/MSF developed a HIL simulator using a 6-

DOF Stewart platform for simulating the Space Shuttle being berthed to the International Space Station (ISS) [1-2]. The Canadian Space Agency (CSA) developed an SPDM Task Verification Facility (STVF) using a 6-DOF, customer-built, hydraulic robot to emulate SPDM performing contact tasks on the ISS [3-5]. German Aerospace Center (DLR) developed a HIL simulation facility called European Proximity Operations Simulator (EPOS) to support satellite rendezvous and docking operations [6-7]. A hybrid facilities used to verify the on-orbit tasks was also developed by Tohoku University [8-9]. What is more, US Naval Research Lab used two 6-DOF robotic arms to emulate satellite rendezvous and capture operations [10]. Recently, NASA JPL used

HIL system to simulate a robotic spacecraft capturing a tumbling asteroid in space [11].

It is known that the ground robots in an HIL simulation facility should have enough bandwidth to track the end-effector's motion of the simulated space robotic system. One way to meet this requirement is to design customer-built robot, as CSA did for the STVF [3], but such a solution is very costly and also time consuming. Another solution is to use modified industrial robots, as DLR did for the EPOS [6].

However, an industrial robot, used as it is, usually does not meet the performance requirements for HIL simulation and thus it must be redesigned and modified. Since significant modifications to an industrial robot require redesign of some major hardware and software components of the robot, which is again very costly and time consuming. Therefore, one has to look for a best balance between achieving a best emulation performance and minimal modifications to the hardware and software of an existing industrial robot.

This paper discusses a solution aimed at making an industrial robot meet the need of HIL simulation of a space manipulator. The proposed solution includes several key points: i) modifies the robot hardware to increase its bandwidth for fast responding to the HIL control commands; ii) creates accurate dynamic model of the industrial robot; iii) uses the dynamic model to compensate the influence of the robot's dynamics to the emulation of the space manipulator and also increase the bandwidth of the emulation robots; iv) implements force control capability for the industrial robot to achieve better responding speed for contact operations.

## 2 OVERVIEW OF THE HIL SIMULATION SYSTEM

The concept of the HIL simulation facility is

schematically shown in Fig.2. It is composed of a space robot operation workstation, a HIL simulation workstation, a space robotic simulator, a real-time parallel computer system, two industrial robots, and an external measurement system including both 3D motion and force sensors. Each component of the system is used to fulfill a particular objective in the HIL simulation process.

The real-time parallel computer unit serves as an integrator of all the other hardware and software components of the HIL simulation system. It achieves real-time simulation by running not only the whole space manipulator's dynamics model and its controllers in real time, but also the process control algorithms for the HIL simulation as well as the high-level control algorithms for the industrial robots.

After the space robot operation workstation and the HIL simulation workstation finishing detections and configurations of the whole system, space robot simulator will compile the tested simulation model and load the codes into the main-controller for the real-time HIL simulation.

The main advances of the HIL simulation facility are:

- i) It uses two partial customized industrial robots which are relatively inexpensive and more reliable in comparison of customer-built robots;
- ii) it allows one of the robots to move on a long rail system to emulate proximity approaching operation;
- iii) it has hardware-in-the-loop, zero-gravity, and contact dynamics simulation capabilities allowing high-fidelity docking and capturing simulation.

Upon all above, the industrial robots play an essential role in achieving the physical contact and tracking the motion behavior of the simulated space robot with high fidelity.

The major specifications of the two industrial robots used in the facility are listed in Table 1.

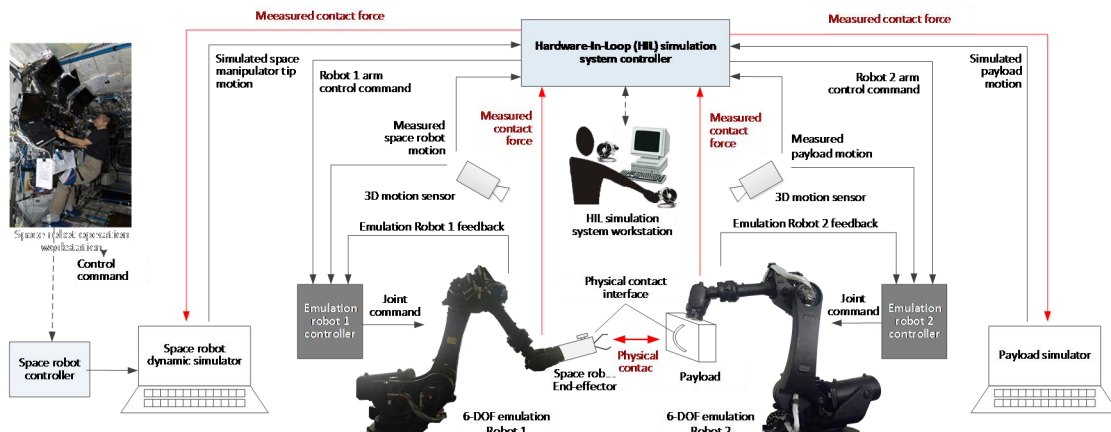


Figure 2: The diagram of the Hardware-in-the-Loop simulation system.

Table 1 Characteristic parameters of the industrial robot used in the simulation facility

Parameters	J1	J2	J3	J4	J5	J6
The maximum static torque (Nm)	0	6400	6000	1650	1650	900
Joint Maximum Speed (°/s)	70	55	60	80	60	100
Joint Motion Range(°)	±180°	+80°~55°	+80°~195°	±360°	±120°	±360°
Maximum Horizontal Reach	2600 mm					
Maximum Load	300 kg					
End-effector mobile repeatability	±0.2mm					

When executing emulation, the two robots are controlled to track the relative motion of the end-effector and that of the payload with respect to the base spacecraft of the space manipulator. When a physical contact happens, the contact force and moment generated by the hardware contact will be measured and fed back to the space robot simulator and the payload simulator. As a result of the input physical contact force and moment, the simulated motions of the space robot and payload will be affected although the simulators do not have a contact dynamics model.

To achieve satisfactory simulation fidelity, it is required that the end-effectors of the two industrial robots behave exactly as the space robot and the payload in space, which means that the industrial robots should be able to respond to the HIL control commands very fast, and dynamically behave like the on-orbit manipulator and payload being simulated, especially when reacting to a physical contact during a contact simulation.

Since industrial robots cannot fully meet the requirements of HIL simulation due to the limited dynamic characteristics, modifications should be made to these robots, which will be described in the next section.

### 3 MODIFICATIONS TO THE INDUSTRIAL ROBOTS

The industrial robots were originally designed for common industrial applications, such as working in an automobile assembly line, often having massive bodies and operating at a sample rate and commanding rate around 100Hz~250Hz. Therefore, the responding time is longer than the requirement of ground verifications for space applications.

What is more, the robots have very different dynamics properties from the space manipulator and payload, as they are basically positioning machines with very high impedance (or very high stiffness when holding on a position). There have been several methods to solve this problem, such as the end-effector admittance

control strategy [7], impedance control strategy [12], the computed torque control [13], passivity-based control [14-15], etc. could control the HIL simulation facility to have realistic contact dynamics simulation.

As can be seen, an accurate dynamics model of the industrial robots, which is not usually available for industrial applications, is the basis of HIL simulation system.

In order to meet the requirements of HIL simulation system, an accurate model of the industrial robots should be established, to compensate the dynamics influence in simulating a space robot; and also, the industrial robots should be enhanced to have bandwidth high enough to response quickly. Besides, the force control mode should also be added to the industrial robots to support the physical contact dynamic emulation.

#### 3.1 Increasing Bandwidth

To increase the bandwidth of an industrial robot for HIL simulation, several modifications may be considered.

The dynamic response of the robot to a given command must be made faster. This can be done by changing the gearboxes to those with a higher gear ratio so that the maximum driving torques will be increased. Industrial manipulators usually demands quick speed in considering efficiency. It is a different story for space robots. To prevent the potential risk of contact force, space robot avoids quick speed during a task. Therefore, the decrease of speed caused by higher gear ratio does no harm for our application.

Joint torque control helps improve the bandwidth of the robot. Thus current-based torque control capability is activated in the robot controller.

The sampling rates of all sensors, especially the force sensor, should be maximized. With careful design, the sampling of velocity and sampling of current is set as 4KHz and 6KHz respectively.

In controlling the joints, industrial robots usually

provide a command rate of no more than 250 Hz. This should be increased also, so that the arm can respond control commands faster. Considering the ability of the hardware, the frequency is set as 1KHz.

On top of these remedies, one can also use an accurate dynamics model of the industrial robot to linearize the dynamics of the hardware robot through a feed-forward unit, so that the feedback for the tracking control will be simplified significantly, and thus improve the bandwidth of the robot.

To estimate the bandwidth of the modified industrial robot, a sinusoidal trajectory was set as the demanded trajectory to be tracked by the end-effector of the robot. Setting the frequency as 1Hz, the amplitude as 20mm, the tracking result with 200Kg payload was shown in Fig.4, where the green dotted line is the demanded trajectory, the blue solid one is the actual trajectory. The tracking error was about 20% of the total amplitude, and the phase shift is around 20 degree, showing that the bandwidth of the modified industrial robot is satisfactory.

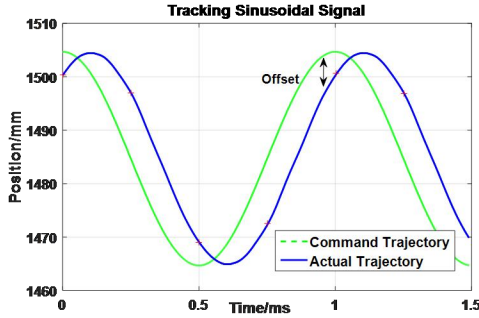


Figure 3: Experiment Result of Tracking an 1Hz Sinusoidal Trajectory

### 3.2 Dynamics Modeling of the Industrial Robot

The dynamics equations of an industrial robot were created based on the rigid body dynamics and physical attributes of the robot. The dynamics of the 6-DOF industrial robot can be described by the following vector equation:

$$\tau = M(q)\ddot{q} + C(q, \dot{q})\dot{q} + G(q) \quad (1)$$

Considering the joint friction model, part of motor's torque will be consumed due to the joint friction and inertia of the rotor, and the rotor inertia will have a significant impact on the dynamic behavior due to the effect of the Coriolis and centrifugal force when rotating rapidly. Taking only the Coulomb friction and viscous friction into consideration, a linearized identification equation of the friction parameters was written as

$$\tau_i^f = f_i^c \text{sign}(\dot{q}_i) + f_i^v \dot{q}_i \quad (2)$$

where  $\tau_i^f$  is the friction-torque;  $f_i^c$  is the Coulomb friction torque;  $f_i^v$  is the viscous friction coefficient.

The rotor inertia can be ignored as it is very small. All parameters in Equation (1) can be grouped into a parameter vector. Adding the friction and rotor inertia parameters, we get a set of linear equations in terms of the model parameters :

$$\tau = \phi_s(q, \dot{q}, \ddot{q})\theta_s \quad (3)$$

where  $\tau$  is the vector of joint torques,  $\phi_s$  is the observation matrix,  $\theta_s$  consists of inertia parameters and friction joint parameters of each joint:

$$\theta_s = [\theta_s^1, \theta_s^2, \dots, \theta_s^N] \quad (4)$$

each element expressed as a vector with 13 elements:

$$\theta_s^i = [I_{xxi}, I_{xyi}, I_{xzi}, I_{yyi}, I_{yzi}, I_{zzi}, mr_{xii}, mr_{yii}, mr_{zii}, m_i, I_a, f_{ci}, f_{vi}]^T \quad (5)$$

In order to accelerate the convergence rate of parameter estimation and noise immunity, the excitation trajectory should be carefully designed, which has been applied to identification experiment repeatedly due to its advantages in signal processing,

Typically, two aspects are considered: i) estimating parameters accurately and fast enough when interference happening; ii) data procession is simple, while result is consistent and accurate enough.

Model error and measurement noise will reduce the accuracy of identification. To obtain, we take the finite terms periodic Fourier series trajectory as the exciting trajectory for the robot, shown as follows:

$$q_i(t) = q_i^0 + \sum_{k=1}^N (a_i^k \cos(k\omega_f t) + b_i^k \sin(k\omega_f t)) \quad (6)$$

where  $q_i^0$  is the compensation of joint position;  $\omega_f$  is the fundamental frequency;  $a_i^k$  and  $b_i^k$  are the coefficient of Fourier series; N is the number of harmonic terms in the Fourier series. Each Fourier series contains 2N+1 parameters, corresponding to  $q_i^0$ ,  $a_i^k$  and  $b_i^k$ , which are the freedom of trajectory optimization with the joint positions, joint velocities, joint accelerations and the motor torques with necessary constraints, such as

$$\begin{aligned} q_{min} &\leq q(\beta) \leq q_{max} \\ \dot{q}_{min} &\leq \dot{q}(\beta) \leq \dot{q}_{max} \\ \ddot{q}_{min} &\leq \ddot{q}(\beta) \leq \ddot{q}_{max} \\ \tau_{min} &\leq \phi(q(\beta), \dot{q}(\beta), \ddot{q}(\beta))\theta \leq \tau_{max} \end{aligned} \quad (7)$$

When the robot tracks a designed excitation trajectory, identification data, including the joint position and the

motor torque converted through the motor current, were sampled and recorded. To overcome the noise of the motor current signal, the collected data preprocessed via periodic averaging.

Instead of obtaining the joint velocities and accelerations through numerical differentiation, an analytical method is employed in two steps: i) fitting Fourier series to the joint position data by least-square method; ii) taking the derivative of the fourier series.

The next step is to estimate the parameters of the robot from the measured data. Realizing the fact that the measurement noises of joint positions are smaller than that of torques, we use weighted least-square method to improve the accuracy of identification. Write the overdetermined equation as

$$\boldsymbol{\tau} = \begin{bmatrix} \tau_1 \\ \tau_2 \\ \vdots \\ \tau_N \end{bmatrix} = \begin{bmatrix} \phi_1(q_1, \dot{q}_1, \ddot{q}_1) \\ \phi_2(q_2, \dot{q}_2, \ddot{q}_2) \\ \vdots \\ \phi_N(q_N, \dot{q}_N, \ddot{q}_N) \end{bmatrix} \boldsymbol{\theta} \triangleq \Phi \boldsymbol{\theta} \quad (8)$$

the parameters can be solved as

$$\hat{\boldsymbol{\theta}} = (\Phi^T \Phi)^{-1} \Phi^T \boldsymbol{\tau} \quad (9)$$

where  $\hat{\boldsymbol{\theta}}$  is the estimated inertia parameter vector.

Three experiments were designed and implemented. The first one results in the estimated inertia parameters after tracking a periodic Fourier series trajectory. The second one verifies the identification result comparing the actual controlling joint torque and the predicated joint torque while tracking another trajectory. Fig.4 presents the comparison of the first joint, which faces the largest torque variation. The comparing results show that the estimate torque has an error of less than 10%.

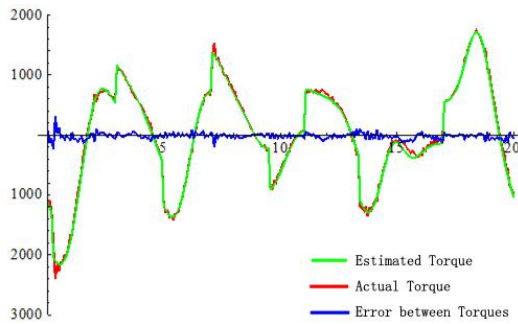


Figure 4: Comparison of the joint torque and the estimated value by the model(joint 1)

The third experiment was to validate the effect of the dynamic feed-forward. Fig.5 shows the tracking error without feed-forward, Fig.6 presents the enhanced result with feed-forward. CH1 presents a demanded velocity, while CH2 shows the actual velocity. Comparison of Fig.5 and Fig.6 show that, the feed-forward unit improves the tracking accuracy and decreases the up-rise, resulting in a quick convergence in the tracking

process.

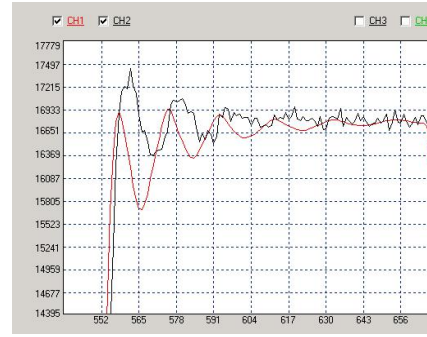


Figure 5: The velocity response without dynamics feed-forward.

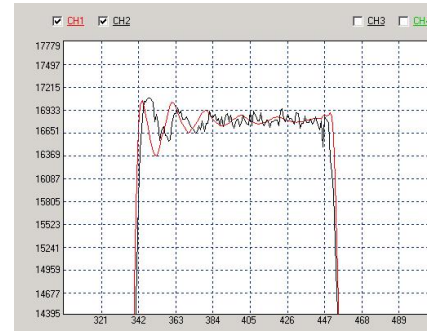


Figure 6: The velocity response in the presence of dynamics feed-forward.

### 3.3 Force Control

According to the reflection between position/velocity and force of the end of robot, force control can be achieved by adjusting the feedback position error, velocity error or stiffness; and when the force fed back is used as not only the position correction but also the velocity correction, that is the impedance control.

To establish the impedance model of the robot between position and force error of the end by using the force error  $E = F_t - F_c$  as the target driving force:

$$M_d(\ddot{X} - \ddot{X}_d) + B_d(\dot{X} - \dot{X}_d) + K_d(X - X_d) = E \quad (10)$$

where  $M_d, B_d, K_d$  are the inertia matrix, damping matrix and stiffness matrix;  $X, \dot{X}, \ddot{X}$  are the position, velocity and acceleration of the end;  $X_d, \dot{X}_d, \ddot{X}_d$  are the target position, velocity and acceleration of the end-effector.

When contact with the environment occurs, the end-effector of the robot, no longer independent, will compound with environment as a comprehensive dynamic system. Usually, the contact model between the manipulator and environmental is simplified as a linear spring system, where the environment can be modeled as a spring-damper system, and the force applied to the end of robot can be described by

$$f_c = k_e(x - x_e) + \dot{x} \quad (11)$$

where  $f_c$  is the contact force between the end of robot and the environment;  $k_e$  is the environmental stiffness;  $x, x_e$  are actual robot position and location of the environment respectively,  $\dot{x}$  is the damping coefficient of environment.

Impedance control based on position is composed of two parts, with the position controller serving as the inner control loop and the impedance controller serving as the outer control loop. The impedance controller generates position correction according to the actual force and the target impedance parameters, and then inputs them to the inner position controller combined with the desired position, making the real position track the desired value, so that the dynamic characteristics of robot can be determined by the

target impedance parameters.

The position correction vector  $X_f$  satisfies the following formulas:

$$M_d \ddot{X}_f + B_d \dot{X}_f + K_d X_f = E \quad (12)$$

$$X_f = \frac{E}{M_d s^2 + B_d s + K_d} \quad (13)$$

Adding to the desired position correction vector  $X_d$  generated by trajectory planning to produce the position control commands  $X_r$  :

$$X_r = X_d + X_f \quad (14)$$

Due to time constraints, it is a pity that the controllers are not yet been fully validated.

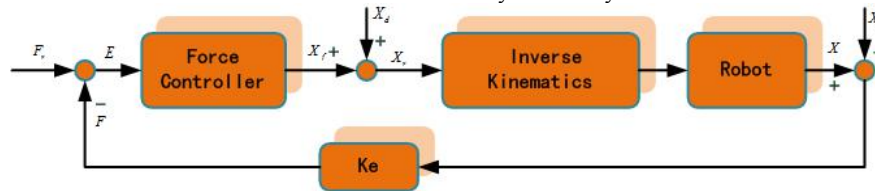


Figure 7 Structure Chart of the Impedance Control

## 4 CONCLUSION

A high-fidelity, hardware-in-the-loop (HIL) simulation facility for simulating a space manipulator performing contact tasks is presented in this paper. The facility uses two customer-modified 6-DOF industrial robots to emulate the relative motions of the space manipulator and its payload. To meet the special requirements for the HIL contact dynamics simulation, the two industrial robots have to be properly modified. The modification includes: i) to broaden the bandwidth of the industrial robot; ii) to establish an accurate dynamic model; iii) to embed force control in the controller. Preliminary simulation validates the effect of these modifications.

What has not been handled till now, which may also affect the simulation results, is the time delay between command and the motion of end-effector. Control scheme

## References

- [1] S. Ananthkrishnan, R. Teders, K. Alder (1996) Role of estimation in realtime contact dynamics enhancement of space station engineering facility, IEEE Robotics Autom. Mag. 3 (3) 20–28.
- [2] F.D. Roe, R.T. Howard, L. Murphy (2004) Automated rendezvous and capture system development and simulation for NASA, in: Proceedings of the SPIE 5420, Orlando, FL, pp. 118–125.
- [3] J.C. Piedboeuf, J. De Carufel, F. Aghili, E. Dupuis (1999) Task verification facility for the Canadian special purpose dexterous manipulator, in: Proceedings of the IEEE International Conference on Robotics and

Automation, Detroit, Michigan, pp. 1077–1083.

- [4] O. Ma, J. Wang, S. Misra, M. Liu (2004) On the validation of SPDM task verification facility, J. Robotic Syst. 21 (5) 219–235.
- [5] F. Aghili, M. Namvar, G. Vukovich (2006) Satellite simulator with a hydraulic manipulator, in: Proceedings of the IEEE International Conference on Robotics and Automation, Orlando, Florida, pp. 3886–3892.
- [6] M. Zebenay, R. Lampariello, T. Boge, and R. Krenn, (2011) “Control Strategy of Hardware-in-the-Loop Simulator EPOS 2.0 for Autonomous Docking Verification”, Proc. in Applied Mathematics and Mechanics.
- [7] O. Ma, A. Flores-Abad, and T. Boge (2012) “Use of industrial robots for hardware-in-the-loop simulation of satellite rendezvous and docking”, Acta Astronautica, Vol. 81(1), pp.335-347.
- [8] K. Yoshida, H. Nakanishi, H. Ueno, N. Inaba, T. Nishimaki, M. Oda (2004) Dynamics, control and impedance matching for robotic capture of a non-cooperative satellite, Adv. Robotics 18 (2) 175–198.
- [9] R. Takahashi, H. Ise, D. Sato (2008) Hybrid simulation of a dual-arm space robot colliding with a floating object, in: Proceedings of the IEEE International Conference on Robotics and Automation, Pasadena, California, pp. 1201–1206.
- [10] R. Bell, T. Morphopoulos, J. Pollack, J. Collins, J.R. Wertz, R.E. Van Allen (2003) Hardware-in-the-loop

tests of an autonomous GN&C system for on-orbit servicing, in: Proceedings of the AIAA-LA Section/SSTC Responsive Space Conference, Kirtland, NM.

- [11] Gates, M., et al. (2015) NASA's Asteroid Redirect Mission concept development summary. 2015 IEEE Aerospace Conference, p.13 pp.-13 pp.
- [12] N. Hogan (1984) "Impedance Control: An Approach to Manipulation", Proc. of American Control Conference, pp.304 - 313.

[13] R. H. Middleton and G. C. Goodwin (1988)"Adaptive computed torque control for rigid link manipulations", Syst. & Ctrl. Letters, Vol. 10(1), pp.9-16.R.

[14] O.A.J. van der Schaft, I. Mareels, and B. Maschke (2001) "Putting energy back in control", IEEE Ctrl. Syst. Mag..

[15] R. Krenn, K. Landzettel, T. Boge, M. Zebenay (2011) Passivity control for hybrid simulations of satellite docking, in: Proceedings of the IEEE International Conference on Robotics and Automation—Space Robotics Workshop, Shanghai, China.